DMD Fast Forward. Published on January 7, 2008 as doi:10.1124/dmd.107.019760
This article has not been copyedited and formatted. The final version may differ from this version.

METABOLISM AND DISPOSITION OF A $GABA_A$ RECEPTOR PARTIAL AGONIST IN HUMANS

Christopher L. Shaffer, Mithat Gunduz[1], Alfin D. Vaz, Karthik Venkatakrishnan[2] and Aaron H. Burstein

Departments of Pharmacokinetics, Pharmacodynamics and Metabolism (C.L.S., M.G., A.D.V.), Clinical Pharmacology (K.V.) and Clinical Research Operations (A.H.B.), Pfizer Global Research and Development, Groton/New London Laboratories, Pfizer Inc., Groton, Connecticut

DMD Fast Forward. Published on January 7, 2008 as DOI: 10.1124/dmd.107.019760
This article has not been copyedited and formatted. The final version may differ from this version.

Running Title: Human Metabolism and Disposition of a $GABA_A$ Partial Agonist

Address correspondence to:

Dr. Christopher L. Shaffer
Pharmacokinetics, Dynamics and Metabolism
Pfizer Global Research and Development
Groton/New London Laboratories
Pfizer Inc.
Eastern Point Road, MS 8220–4186
Groton, CT 06340
Tel. 860.441.3377
Fax 860.686.6532
Email: Christopher.L.Shaffer@pfizer.com

Text pages: 28
Tables: 8
Figures: 3
References: 29
Words in Abstract: 162
Words in Introduction: 324
Words in Discussion: 1,235

Abbreviations: $GABA_A$, γ-aminobutyric acid type-A receptor; **1**, *N*-[3-fluoro-4-[2-(propylamino)ethoxy]phenyl]-4,5,6,7-tetrahydro-4-oxo-1*H*-indole-3-carboxamide monomethanesulfonate; **2**, 2-fluoro-4-[(4-oxo-4,5,6,7-tetrahydro-1*H*-indole-3-carbonyl)-amino]-phenoxy acetic acid; **3**, 4-oxo-4,5,6,7-tetrahydro-1*H*-indole-3-carboxylic acid [3-fluoro-4-(2-hydroxy-ethoxy)-phenyl]-amide; [^{14}C]**1**, *N*-[3-fluoro-4-[2-(propylamino)ethoxy]phenyl]-4,5,6,7-tetrahydro-4-oxo-1*H*-[3-^{14}C]indole-3-carboxamide monomethanesulfonate; HLM(s), human liver microsome(s); P450(s), cytochrome(s) P450; MAO, monoamine oxidase; HPLC, high-performance liquid chromatography; LC-MS/MS, liquid chromatography-tandem mass spectrometry; LLOQ, lower limit of quantification; AUC, area under the plasma concentration-time curve; k_{el}, elimination rate constant; rcf, relative centrifugal force; LSC, liquid scintillation counting; MRM, multiple-reaction monitoring; NADPH, reduced β-nicotinamide adenine dinucleotide phosphate; LC t_R, liquid chromatography retention time; CID, collision-induced dissociation; GFR, glomerular filtration rate.

Abstract

The metabolism and disposition of *N*-[3-fluoro-4-[2-(propylamino)ethoxy]phenyl]-4,5,6,7-tetrahydro-4-oxo-1*H*-indole-3-carboxamide (**1**), a potent subtype-selective partial agonist at the $GABA_A$ receptor complex, were elucidated in humans following an oral dose of [^{14}C]**1**. Overall, **1** was well tolerated, with approximately twice as much radioactivity excreted in feces (64.8%±13.3%) as in urine (28.4%±8.8%). Across subjects, the oral clearance of **1** was comprised of both renal (10%) and metabolic (≤90%) components, with the biotransformation of **1** happening predominately via oxidative deamination to either carboxylic acid **2** or alcohol **3**, and minimally by aliphatic hydroxylation and carbamate formation. Active renal secretion of **1** was observed as its unbound renal clearance was six-fold greater than the glomerular filtration rate. Experiments using human hepatic *in vitro* systems were undertaken to better understand the enzyme(s) involved in the clinically observed oxidative biotransformation pathways. *N*-Dealkylation of **1**, the principal metabolic route observed *in vivo*, was found to be predominately MAO-B-mediated with the resulting putative aldehyde intermediate undergoing subsequent oxidation to **2** or reduction to **3**.

DMD Fast Forward. Published on January 7, 2008 as DOI: 10.1124/dmd.107.019760
This article has not been copyedited and formatted. The final version may differ from this version.

Introduction

Generalized Anxiety Disorder (GAD) is one of the most prevalent psychiatric illnesses (Kessler et al., 1994) causing sizeable societal costs in terms of a patient's considerably lower quality of life relative to the general population and economic repercussions measured by lost productivity and the requirement for extensive healthcare resources (Wittchen, 2002; Lieb et al., 2005; Jorgensen et al., 2006). Benzodiazepines are most commonly prescribed for the treatment of GAD although they exhibit many side effects such as sedation, cognitive impairment, withdrawal and abuse liability (Lader, 1994; Woods and Winger, 1995; Rickels and Rynn, 2002). Other medicines, like buspirone (Lader, 1988) and selective serotonin (or serotonin-norepinephrine) reuptake inhibitors (Brawman-Mintzer et al., 2006; Lam, 2006; Simon et al., 2006), have been identified as safer alternatives to benzodiazepines for treating GAD, but often lack the rapid and robust efficacy of the benzodiazepines.

Benzodiazepines exert their efficacy in a full-agonist fashion by allosterically modulating the $GABA_A$ receptor complex (Olsen and Tobin, 1990; Drexler et al., 2006), which potentiates GABA-mediated neuronal inhibition (Sieghart, 1992; Mohler et al., 2002). Unlike full agonists, partial agonists of the $GABA_A$ receptor, particularly those that are subtype selective (Low et al., 2000; Mohler et al., 2002; Griebel et al., 2003), may afford concurrently the desired anxiolytic effects of a benzodiazepine while minimizing or eliminating its unwanted side effects resulting in a superior safety profile for the general and chronic treatment of GAD (Lader, 1994).

N-[3-Fluoro-4-[2-(propylamino)ethoxy]phenyl]-4,5,6,7-tetrahydro-4-oxo-1*H*-indole-3-carboxamide (**1**), a potent subtype-selective partial agonist at the $GABA_A$

DMD Fast Forward. Published on January 7, 2008 as DOI: 10.1124/dmd.107.019760
This article has not been copyedited and formatted. The final version may differ from this version.

receptor complex, elicits anxiolytic effects in rats without the side effects of benzodiazepines (unpublished Pfizer Inc. internal data). The study reported herein was undertaken to ascertain definitively the metabolic and excretory pathways of **1** in humans following a single oral dose of [^{14}C]**1** (Figure 1). Determination of the clearance routes, metabolites and pharmacokinetics of **1** in the clinic has provided deeper insight into its overall human disposition, and confirmed rats and monkeys as appropriate toxicological species (Shaffer et al., 2005).

Materials and Methods

Chemicals and Reagents. Compounds **1**, **2** and **3** were provided by Neurogen Corp. (Branford, CT); [^{14}C]**1** (50.7 mCi/mmol, 99.0% radiochemical purity) was made by the Radiochemical Synthesis Group at PGRD (Groton, CT). The chemical purity of all synthetic compounds was >99%. HLMs (17.6 mg protein/mL, 0.32 nmol P450/mg protein), pooled from 53 individual donors, and human liver mitochondria (20 mg protein/mL) were purchased from XenoTech LLC (Lenexa, KS). Cryopreserved human hepatocytes (from three donors) were procured from In Vitro Technologies Inc. (Baltimore, MD). Recombinant human MAO-A (20 mg protein/mL) and MAO-B (20 mg protein/mL) membranes were provided by Prof. Dale E. Edmondson under contract with Pfizer Inc. Chemicals and solvents of reagent or HPLC grade were supplied by Aldrich Fine Chemical Co. (Milwaukee, WI), Fisher Scientific (Pittsburgh, PA) and the J. T. Baker Chemical Co. (Phillipsburg, NJ). TruCount liquid scintillation cocktail was purchased from IN/US Systems, Inc. (Tampa, FL). All excreta and plasma were collected gravimetrically and stored at –20 °C until analysis.

Dosing of Human Volunteers and Collection of Samples. The study was a non-randomized, open-label, single-dose study to investigate the absorption, metabolism and excretion of **1** in humans. The study population was comprised of six healthy, non-smoking adult white male volunteers between the ages of 18 and 64 years and weighing 61 to 91 kg. The study was conducted in compliance with an Institutional Review Board (IRB)/Independent Ethics Committee, informed consent regulations and ICH GCP Guidelines. The IRB approved both the study protocol and informed consent documents prior to drug shipment. After being informed of the design, purpose and potential risks of

DMD Fast Forward. Published on January 7, 2008 as DOI: 10.1124/dmd.107.019760
This article has not been copyedited and formatted. The final version may differ from this version.

the study, written informed consent was required from each subject prior to their enrollment at the PPD Phase 1 Clinic (Austin, TX), where they were kept under continuous medical surveillance from 24 h pre-dose to 264 h post-dose. Subjects were required to fast 8 h before and 4 h after dosing. Each subject was administered 200 mg (ca. 91 μCi) of [^{14}C]**1** dissolved in sterile H_2O (100 mL), which was swallowed directly from a 30 cc wide-mouth amber glass dosing bottle, followed by more sterile H_2O (two 70 mL bottle rinses).

From each subject, urine was collected pre-dose and from 0–12 and 12–24 h during Day 1, and in 24 h intervals from 24–240 h post-dose, while feces were collected pre-dose and as passed at 24 or 48 h intervals for 11 days post-dose. Blood samples sufficient to provide 5 mL of plasma were collected into sodium heparinized tubes via arm venipuncture pre-dose and at 0.5, 1, 2, 4, 8, 12, 24, 48, 72, 96, 120, 144, 168, 192, 240, 264, 288 and 312 h post-dose for the pharmacokinetic evaluation of **1** and total radioactivity; having been released from the Clinic on Day 11 (264 h post-dose), subjects returned to the Clinic for the 288 and 312 h post-dose blood draws. Blood samples sufficient to provide 20 mL of plasma were collected similarly at 1, 4, 8, 12 and 24 h post-dose for the profiling of metabolites of **1**. Control plasma was harvested from pre-dose blood samples.

Determination of Radioactivity within Biological Matrices. Triplicate gravimetric aliquots (0.1 g) of each sample of urine and plasma were mixed with TruCount scintillation cocktail (7 mL) and counted for 4 min in a model LS 6500 liquid scintillation counter (Beckman Coulter, Fullerton, CA). Fecal samples were homogenized with distilled H_2O (ca. 20% w/w, feces/H_2O) using a Stomacher homogenizer. Triplicate

DMD Fast Forward. Published on January 7, 2008 as DOI: 10.1124/dmd.107.019760
This article has not been copyedited and formatted. The final version may differ from this version.

gravimetric aliquots (0.5–0.7 g) of fecal homogenate were transferred into tared cones and pads, weighed, dried for a minimum of 24 h at ambient temperature and combusted by a Packard Instruments Model A0387 sample oxidizer (Packard BioScience, Co., Meriden, CT). Combustion efficiency using a ^{14}C standard was determined daily before the combustion of study samples, and the measured radioactivity content in feces was adjusted using daily combustion efficiency values. The resulting [^{14}C]CO_2 was trapped in Monophase-S® (Perkin Elmer Life and Analytical Sciences, Boston, MA), mixed in Perma-Fluor-E scintillation fluid (Packard BioScience, Co., Meriden, CT) and quantified over 10 min in a Packard Instruments Model 2300 liquid scintillation counter (Packard BioScience, Co., Meriden, CT). Scintillation counter data were automatically corrected for counting efficiency using an external standardization technique and an instrument-stored quench curve generated from a series of sealed quench standards.

Quantitative Analysis of 1 in Plasma. Plasma concentrations of **1** for each subject were determined using a validated LC-MS/MS assay (Venkatakrishnan et al., 2007) at MDS Pharma Services (Lincoln, NE). The dynamic range of the assay was 1–1,000 ng/mL for **1**.

Calculations. Pharmacokinetic parameters were calculated for each subject by non-compartmental analyses using WinNonlin Version 3.2 (Pharsight Corp., Mountain View, CA). Values used to determine the pharmacokinetic parameters of total radioactivity were calculated by converting the LSC-generated raw data to concentrations (ng-eq./mL) using the specific activity (0.17 mCi/mmol) of administered [^{14}C]**1**. The $AUC_{0-tlast}$ was calculated using the linear trapezoidal method, k_{el} was determined by linear regression of the log concentration versus time data during the terminal phase, half-life ($t_{1/2}$) was

calculated as (ln2)/k_{el} and $AUC_{0-\infty}$ was calculated as the sum of $AUC_{0-tlast}$ and $AUC_{tlast-\infty}$, which was determined by dividing the plasma concentration at t_{last} by k_{el}. Both maximal plasma concentration (C_{max}) and its time of first occurrence (T_{max}) were taken directly from the concentration versus time data. Means and standard deviations were calculated when half or greater of the values exceeded the LLOQ for **1** (1.0 ng/mL) or total radioactivity (72.7 ng-eq./mL). A value of 0 was used when a measured concentration was below its LLOQ. For each subject, oral plasma clearance (CL_p/F) of **1** was calculated by dividing the dose by respective plasma $AUC_{0-\infty}$, and renal clearance (CL_R) of **1** was calculated by dividing the amount of **1** excreted unchanged in urine over 48 h (Ae_{0-48}), as determined by the radioprofiling of pooled individual urine (see below), by its plasma AUC_{0-48}; both clearance values were then subject weight-normalized to afford units of mL/min/kg. The use of urinary excretion data collected over 48 h post-dose for CL_R calculations is justified as being ca. five times the estimated $t_{1/2}$ of **1** in this study.

Sample Preparation for Metabolite Profiling and Identification. At each step during the sample preparation of all biological matrices, total radioactivity levels were determined by LSC for recovery calculations. Following preparation, all samples were analyzed as described below by LC-MS/MS with radiometric detection. Pre-dose and blank samples served as controls for determining background radioactivity and endogenous, non-drug-related ions observed within respective matrices or their extracts by LC-MS/MS.

Urine. Urine samples from each subject collected from 0–48 h post-dose representing >95% of total urine radioactivity were pooled proportional to the amount of urine in each sampling period for analysis by LC-MS/MS with radiometric detection.

DMD Fast Forward. Published on January 7, 2008 as DOI: 10.1124/dmd.107.019760
This article has not been copyedited and formatted. The final version may differ from this version.

Pooled urine samples (13–30 mL) were concentrated by a N_2 stream at 37 °C, reconstituted in 1% isopropanol in 2 mM ammonium acetate, pH 4.3 (0.5 mL, Solvent A) and centrifuged (832 rcf for 10 min) to afford the analytical sample, which retained ≥90% of the radioactivity contained within the pooled sample prior to concentration.

Feces. Fecal homogenates from each subject were pooled based on sample time intervals representing >90% of total fecal radioactivity, and were pooled for analysis as described above for urine. Pooled fecal homogenates (7–10 g) were diluted with H_2O (1 mL/g homogenate) and agitated at 37 °C overnight in a shaking water bath. The softened stool samples were diluted with MeCN (2 mL/g homogenate), vortex-mixed and centrifuged (832 rcf for 10 min) and the resulting supernatant was transferred to a clean vial. The remaining fecal pellets were extracted an additional one or two times with 33% H_2O in MeCN (9 mL) to ensure that >90% of radioactivity, as determined by LSC analysis of the combined supernatants, from each pooled fecal sample was extracted. The combined supernatants were concentrated by a N_2 stream at 37 °C and reconstituted in Solvent A (2 mL) to yield the analytical sample, which retained ≥90% of the radioactivity contained within the pooled sample prior to concentration.

Plasma. Plasma from blood samples drawn from each individual at 1, 4, 8, 12 and 24 h post-dose were used for circulatory metabolite profiling and identification; these time points accounted for 100% of the total radioactivity AUC since for all subjects the last quantifiable time point for radioactivity was 24 h post-dose. Plasma samples were pooled according to the method of Hamilton *et al.* (Hamilton et al., 1981); i.e. 2, 3.5, 4, 8 and 6 mL, respectively, of plasma from each time point were combined. To remove dissolved proteins, pooled plasma samples (23.5 mL) were diluted with MeCN (47 mL), vortex-

mixed and centrifuged (3,661 rcf for 10 min), and the resulting supernatants, which contained >90% of the radioactivity from each pooled sample, were isolated. Each supernatant was concentrated to near dryness at 35 °C under N_2 and reconstituted in Solvent A (250 μL) to provide the analytical sample.

Metabolite Profiling and Identification. Samples were analyzed by an LC-MS/MS system comprised of a PE Sciex API-3000 tandem quadrupole mass spectrometer with a TurboIonSpray® interface (Perkin Elmer Life and Analytical Sciences, Boston, MA), two Shimadzu LC-10A HPLC pumps (Shimadzu USA, Columbia, MD) and a CTC PAL Autosampler (LEAP Technologies, Carrboro, NC), in series with a β-RAM radiometric detector (IN/US Systems, Inc.) containing a liquid scintillant cell (250 μL). Analytes within sample aliquots (25–100 μL) were eluted on a Column Engineering Monitor C_{18} analytical column (5 μ, 4.6 × 150 mm) at 1 mL/min with solvent A and MeCN (Solvent B). The following two-step gradient was employed: 0 to 45 min, 5% to 60% solvent B in solvent A; 45 to 50 min, 60% to 80% B in A. Following the elution of **1** and its metabolites, the column was washed with 80% B in A for 2 min and then returned over 3 min to 5% B in A where it remained for 10 min prior to the next injection. For each matrix, >94% of the radioactivity injected onto the column eluted during the first 40 min of the gradient program. HPLC effluent was split 1:9 between the mass spectrometer and the radiometric flow detector; liquid scintillation cocktail flowed at 3 mL/min to the radiometric detector. Mass spectral data were collected using positive ionization in full, precursor ion, neutral loss, product ion and MRM scanning modes. Instrument settings and potentials were adjusted to provide optimal data in each mode. Masschrom version 1.1.1 (Perkin Elmer Life and Analytical Sciences) and Winflow version 1.4 (IN/US

Systems, Inc.) software were used for the acquisition and processing of mass spectral and radiochromatographic data, respectively.

Since the radioactivity in all reconstituted plasma samples was too low for quantification by radiometric flow detection, HPLC effluent was isolated in 30 s intervals by a Gilson FC 204 fraction collector (Gilson, Inc., Middleton, WI), and each respective fraction was mixed with scintillation fluid (7 mL) and subjected to LSC for 5 min. Individual plasma radiochromatograms were generated from respective liquid scintillation data using Microsoft Excel® (Microsoft Office 2000® 9.0.4402 SR-1) and paired with their respective MRM chromatograms.

***In Vitro* Incubations with [^{14}C]1.** All samples from incubations using [^{14}C]**1** were analyzed by the LC-MS/MS with radiometric detection system described previously; in-line radiodetection quantified **1** and its metabolites, whose identification was confirmed by previously observed LC t_Rs and CID spectra.

Human Liver Microsomes. To determine NADPH-dependent metabolites, incubations (2.5 mL) were first performed in duplicate with NADPH (3.3 μmol) in 10 mL Erlenmeyer flasks open to air at 37 °C in a shaking water bath. Each incubation contained HLMs (1.5 mg of protein/mL 0.1 M KH_2PO_4 buffer, pH 7.4), $MgCl_2$ (7.5 μmol), and [^{14}C]**1** (50 nmol, 5.1 nCi/nmol). Sample aliquots (1 mL) were removed by micropipette at 0 and 60 min after NADPH addition, quenched with MeCN (5 mL), centrifuged (1,509 rcf for 5 min) and the resulting supernatant concentrated and reconstituted in solvent A (0.5 mL) for LC-MS/MS analysis. To determine non-NADPH-dependent metabolites of **1**, incubations were performed as described above but lacked NADPH and sample aliquots were taken at 0 and 4 h after addition of [^{14}C]**1**. For HLM

incubations with metabolites **2** and **3**, 1 h incubations (±NADPH) were conducted in duplicate.

Human Hepatocytes. Incubations (2.5 mL), which were gassed every hour with 5% CO_2 in O_2, were performed in duplicate in capped 10 mL Erlenmeyer flasks at 37 °C in a shaking water bath. Each incubation contained thawed cryopreserved human hepatocytes (2×10^6 viable cells/mL bicarbonate-based Williams's E-media with 10% FBS) and [^{14}C]**1** (50 nmol, 5.1 nCi/nmol). A sample aliquot (0.5 mL) was removed by micropipette just after addition of **1** and quenched with MeCN (1 mL). After 4 h of reaction, the incubation was terminated with MeCN (4 mL). Quenched samples were vortex-mixed and centrifuged (1,509 rcf for 5 min), and the resulting supernatant was evaporated under N_2 at 35 °C and the residue was reconstituted in solvent A (0.1 to 0.5 mL) for LC-MS/MS analysis.

Human Liver Mitochondria. Incubations (2 mL) were performed in duplicate using the apparati employed for HLMs. Each incubation contained human liver mitochondria (1 mg protein/mL 0.1 M KH_2PO_4 buffer, pH 7.4) and [^{14}C]**1** (40 nmol, 5.1 nCi/nmol). Incubations were terminated by the addition of MeCN (4 mL) 3 h after substrate addition, and the duplicate incubations were combined to optimize analytically the total amount of radioactivity within ultimate sample aliquots. Quenched incubations were processed as described earlier to afford the analytical supernatant for LC-MS/MS analysis.

***In Vitro* Studies Investigating the MAO-mediated Conversion of 1 to 2 and 3.** All samples from incubations using non-radiolabeled **1** were analyzed by an LC-MS/MS system consisting of a TSQ Quantum triple quadrupole mass spectrometer with an

electrospray ionization source (Thermo Fisher Scientific, Inc., Waltham, MA), a Series 1100 HPLC pump with membrane degasser and an autosampler (Agilent Technologies, Inc., Santa Clara, CA). Analytes within sample aliquots (50 μL) were eluted on a Phenomenex Luna C_{18} analytical column (5 μ, 2.0 × 50 mm) at 0.5 mL/min with 5 mM ammonium formate, pH 3.0 (Solvent C) and solvent B using the following gradient: 0 to 2 min, 25% B in C (effluent diverted to waste); 2 to 4 min, 25% to 90% B in C; 4 to 6 min, 90% B in C. Upon elution of **1**, **2**, and **3**, the column was returned over 0.5 min to 25% B in C where it remained for 2.5 min before the next injection. Instrument settings and potentials were adjusted to provide optimal data. Mass spectral data were collected using positive ionization in MRM scanning mode monitoring *m*/z 374.0→162.0 (**1**, LC t_R = 2.6 min), *m/z* 347.0→162.0 (**2**, LC t_R = 4.6 min), and *m/z* 333.0→162.0 (**3**, LC t_R = 4.8 min); monitored ions were windowed by ±0.7 amu. Quantification of **1**, **2**, and **3** were accomplished using standard curves ranging from 10 to 1,000 nM. LCQuan (Thermo Fisher Scientific, Inc.) software was used for the acquisition and processing of mass spectral data.

Recombinant Human MAO-A and MAO-B Membranes. To determine more precisely the MAO-A and/or MAO-B contributions to, and kinetics for, the metabolism of **1** to **2** and **3**, incubations (1 mL) were performed in duplicate in 1.4 mL polypropylene microtubes open to air at 37 °C in a shaking water bath. Each incubation contained either MAO-A or MAO-B membranes (10 μg of protein/mL 50 mM KH_2PO_4 buffer, pH 7.4) and **1** (20 nmol). Sample aliquots (100 μL) were removed by micropipette at 0, 10, 20, 30, 40, 50, 60 and 70 min after addition of **1**, quenched with 10% formic acid in MeCN (500 μL) containing an internal standard, vortex-mixed and then filtered through a

DMD Fast Forward. Published on January 7, 2008 as DOI: 10.1124/dmd.107.019760
This article has not been copyedited and formatted. The final version may differ from this version.

Millipore mixed cellulose ester membrane (0.45 μ). Filtrates were evaporated to dryness under a N_2 stream at 37 °C, and the resulting residues were reconstituted in 10% MeCN in H_2O (100 μL) and analyzed by LC-MS/MS as described previously.

DMD Fast Forward. Published on January 7, 2008 as DOI: 10.1124/dmd.107.019760
This article has not been copyedited and formatted. The final version may differ from this version.

Results

Clinical Observations. Six healthy, adult male volunteers were enrolled as planned. All subjects completed the study and were evaluable for adverse events, safety laboratory tests and pharmacokinetics. There were no serious adverse events, withdrawals due to adverse events or deaths associated with this study. Following administration of **1**, the only reported adverse event was diarrhea in one subject. There were no vital signs, electrocardiogram or safety laboratory test findings of potential clinical concern. Overall, **1** was well tolerated.

Excretion of Total Radioactivity. Mean overall recovery of excreted drug-derived material (Table 1) was 93.2%±14.3%, with approximately half as much radioactivity in urine (28.4%±8.8%) as in feces (64.8%±13.3%). Although ≥94% of administered radioactivity was recovered from five of the subjects over the study period, collected excreta accounted for only 64.5% of the dose given to Subject 4, an obvious outlier within the study group. Interestingly, urinary recovery for Subject 4 (22.4%) was consistent, while fecal recovery (42.1%) was inconsistent, with that of the other five subjects (29.6%±9.3% and 69.4%±8.2%, respectively). This discrepancy is manifested in a larger SD in the mean fecal and total recoveries including Subject 4; mean urinary recovery SD is essentially unaffected by Subject 4. Similarities in both urinary recovery and pharmacokinetics (for both **1** and total ^{14}C) for Subject 4 relative to all other subjects suggest this volunteer's much lower overall recovery was most likely due to deficient fecal collection rather than partial dose ingestion. The excretion rate of total drug-related material was moderate in all subjects; on average, >80% of the recovered radioactivity was excreted within 4 days post-dose.

DMD Fast Forward. Published on January 7, 2008 as DOI: 10.1124/dmd.107.019760
This article has not been copyedited and formatted. The final version may differ from this version.

Pharmacokinetics of 1 and Total Radioactivity. Raw data for determining the pharmacokinetic parameters of **1** and total radioactivity were acquired using a validated LC-MS/MS assay and LSC, respectively. In all subjects, concentrations of **1** and total radioactivity were below their individual LLOQ within plasma sampled beyond 48 h and 24 h post-dose, respectively, defining these time points as respective T_{last} values. For **1** and total radioactivity, mean plasma concentrations vs. time are plotted in Figure 2, and mean pharmacokinetic parameters are listed in Table 2.

Structural Rationalization of 1 and Its Metabolites. Compound **1** had a protonated molecular ion of *m/z* 374 and an LC t_R of ca. 19.8 min; its CID product ion spectrum contained fragment ions with *m/z* 271, 213, 193, 180, 162 and 86 (Figure 1, Table 3). Precursor ion scanning of diagnostic fragment ions *m/z* 162 and 213 determined if metabolites of **1** were modified on either its 4-oxotetrahydroindole or aniline moiety, respectively. A summary of all metabolite LC-MS/MS data is found in Table 3.

The identification of a metabolite as a fully characterized synthetic standard (i.e. **2** or **3**) was determined by the compounds' indistinguishable CID spectra and LC t_R. Metabolites **M1**, **M2**, **M3**, **M4**, **M5** and **M7**, for which authentic standards did not exist, were each assigned a tentative structure based on their respective *m/z*, precursor ion scan response and CID spectrum. Unknown metabolites **U1** and **U2** were not assigned even a speculative structure since neither ionized within the MS in either positive or negative ion mode, which precluded generation of any mass spectral data. Due to extremely limited remaining plasma quantities following circulatory radioprofiling and the inability to form **U1** or **U2** *in vitro*, no further analyses were conducted for the structure elucidation of either metabolite.

DMD Fast Forward. Published on January 7, 2008 as DOI: 10.1124/dmd.107.019760
This article has not been copyedited and formatted. The final version may differ from this version.

Quantitative Profile of [^{14}C]1 and Its Metabolites in Excreta and Plasma.

Unchanged **1** and metabolite **2** were the only compounds observed in the urine of all subjects, while metabolites **U1**, **U2**, **M1**, **M2**, **M4** and **M5** were detected in at least half of the six volunteers (Table 4). On average, 9.9%±2.6% of administered **1** was renally excreted (Table 2). Unchanged **1**, **M1**, **2**, **M4** and **M5** were detected in the feces of all subjects, while **3** and **M2** were observed for five and two subjects, respectively (Table 5). Regardless of subject, **2** was the predominate metabolite in both excretory matrices. In plasma, **1**, **U1**, **M2**, **2**, **M4** and **3** were observed in all subjects; **U2** and **M7** were observed in five (Table 6). On average, **1** comprised 19.1%±4.2% of total circulatory radioactivity in humans, consistent with the mean pharmacokinetic-derived AUC_{0-24} ratios for **1** and total radioactivity of 30.9%±6.0%.

***In Vitro* Metabolism of 1.** Following identification of the human *in vivo* metabolites of **1**, experiments using human liver-derived *in vitro* systems and [^{14}C]**1** were first undertaken to identify the hepatic subcellular fraction(s) responsible for the oxidative deamination of **1**, the most clinically relevant metabolic clearance pathway identified in the human mass balance study with [^{14}C]**1**. The use of [^{14}C]**1** in the initial leg of these studies permitted both the direct quantification of **1** and its metabolites without the need for analytical calibration curves, as well as the detection of non-ionizable metabolites **U1** and **U2** (if formed *in vitro*). Although the enzymology underlying the conversion of **1** to **2** and **3** was of greatest interest based on the human *in vivo* metabolite profiles from a quantitative perspective, the general enzyme identification for all metabolic pathways was undertaken.

DMD Fast Forward. Published on January 7, 2008 as DOI: 10.1124/dmd.107.019760
This article has not been copyedited and formatted. The final version may differ from this version.

For studies using [^{14}C]**1** (Table 7), HLMs converted ca. 39% of **1** to **M1**, **2**, **3** and **M5** in the presence of NADPH; in the absence of NADPH, HLMs transformed ca. 49% of **1** to **2** and **3** only. These data suggested that the HLM-mediated formation of **M1** and **M5** was NADPH-dependent, while that of **2** and **3** was predominately not NADPH-dependent. A combination of the oxidative deamination of **1**, ultimately affording **2** and **3**, being a largely NADPH-independent metabolic clearance pathway in HLMs and reports (Jarrott and Iversen, 1968; Unzeta et al., 1983; unpublished Pfizer Inc. internal data) that liver microsomes are often contaminated with MAO, suggested MAO was the culprit of the *N*-dealkylation of **1**. In human hepatocytes, **1** formed **2** and **3** only following ca. 60% consumption of **1**, once again suggesting the role of MAO in the oxidative deamination of **1**. Next, human liver mitochondria, the hepatic organelle containing the vast majority of MAO (Testa, 1995b), metabolized **1** to **2** and **3** only (Table 7), further validating **1** as an MAO substrate. In no tested human hepatic-derived *in vitro* systems using [^{14}C]**1** were **U1** or **U2** observed.

Based on the *in vitro* metabolism studies conducted with [^{14}C]**1**, recombinant human MAO-A and MAO-B membranes were employed to determine more precisely the MAO-A and/or MAO-B contributions to and preliminary rates of the oxidation of **1** to **2** and **3** (Table 8). In the MAO-A membrane system, **1** was converted minimally to **2** and **3** at equivalent rates (ca. 0.56 pmol metabolite/min/mg). In the MAO-B membrane system, **1** was also metabolized to both **2** (3.1 pmol **2**/min/mg) and **3** (31.8 pmol **3**/min/mg), but at formation rates five- to sixty-fold greater, respectively, than those observed in the MAO-A system (Table 8).

DMD Fast Forward. Published on January 7, 2008 as DOI: 10.1124/dmd.107.019760
This article has not been copyedited and formatted. The final version may differ from this version.

***In Vitro* Metabolism of 2 and 3.** Incubation of **2** and **3** with HLMs for purely qualitative purposes afforded **M4** and **M5**, respectively, in an NADPH-dependent manner; no other metabolites were observed for either **2** or **3**.

DMD Fast Forward. Published on January 7, 2008 as DOI: 10.1124/dmd.107.019760
This article has not been copyedited and formatted. The final version may differ from this version.

Discussion

The metabolism and disposition of **1** were quantitatively characterized in humans following a single oral dose of [^{14}C]**1** (200 mg, 91 μCi), which was well tolerated in all six healthy volunteers. Mean overall recovery of administered radioactivity was 93.2%±14.3%, with approximately twice as much in feces (64.8%±13.3%) as in urine (28.4%±8.8%). The excretion rate of total drug-related material was moderate in humans with >80% of the recovered radioactivity excreted within 4 days post-dose. A combination of short T_{max} for both **1** and total ^{14}C, sizeable amounts of urinary radioactivity, and the predominance of non-microflora-generated metabolites within feces suggested **1** was rapidly and substantially (≥76% of dose) absorbed orally in humans. Across subjects, the oral clearance of **1** was comprised chiefly of metabolic components with only minimal renal clearance (ca. 10%). The precise metabolic contribution to oral clearance is unknown since noteworthy fecal amounts (ca. 14% of dose) of **1** suggested a possible biliary component to its oral clearance. However, the size of this contribution was undeterminable since it was unknown how much of **1** (if any) detected in feces was actually absorbed following ingestion. Biliary clearance of **1** was minimal in both rats and monkeys (Shaffer et al., 2005).

Approximately 10% of administered **1** was excreted unchanged in urine, equal to the pharmacokinetically-derived contribution of renal clearance (CL_R) to apparent oral clearance (CL_p/F) (Table 3). Active renal secretion of **1** was observed as its unbound CL_R was six-fold greater than the glomerular filtration rate (GFR) (Table 3), consistent with the identification of **1** as a MDR1 P-glycoprotein substrate (Venkatakrishnan et al., 2007) and the established contribution of this transporter to active renal secretion of its

substrates (Lee and Kim, 2004). A similar extent of active renal secretion was observed in monkeys (6× GFR), but not rats (2× GFR) (Shaffer et al., 2005).

Overall, qualitatively and quantitatively similar metabolite profiles in all biological matrices were observed across subjects (Tables 4–6). A proposed schematic overview of the human metabolism of **1** is presented in Figure 3. Based on the identification of all urinary and circulatory metabolites, other than **U1** and **U2**, human biotransformation of **1** occurs predominately via *N*-dealkylation, which has been demonstrated *in vitro* to be mediated predominately by MAO-B, with only minor contributions by MAO-A or P450(s). The resulting putative aldehyde undergoes one of two facile fates: oxidation to **2** or reduction to **3**. *In vitro* experiments suggest **2** and **3** each undergo P450-catalyzed hydroxylation to **M4** and **M5**, respectively. The enzymes suspected in the conversion of the aldehyde intermediate to **2** and **3** are ALDH and ADH, respectively, both of which are found in hepatocytes as well as hepatic microsomes, cytosol and mitochondria (Testa, 1995a), and consistent with the presented observations. Interestingly, HLMs may have greater intrinsic reductive (versus oxidative) capacity of the putative aldehyde intermediate since greater quantities of **3** relative to **2** were observed in HLMs (±NADPH) than in either hepatocytes or liver mitochondria (Table 7). However, the observation of considerable quantities of **2** and **3** in HLM incubations lacking NADPH, which itself and its oxidized form ($NADP^+$) could act as respective cofactors for ALDH and ADH within NADPH-containing HLM incubations, does suggest that the formation mechanisms of **2** and **3** from their common aldehyde precursor in cofactor-free HLMs are unresolved redox quandaries. Conversely, three-fold greater quantities of **2** versus **3** observed in both hepatocytes and liver mitochondria (Table 7)

DMD Fast Forward. Published on January 7, 2008 as DOI: 10.1124/dmd.107.019760
This article has not been copyedited and formatted. The final version may differ from this version.

were more indicative of the clinical excretory metabolic profiles suggesting these *in vitro* systems may contain most appropriately the necessary cofactors for both ALDH (NAD^+) and ADH (NADH), facilitating conversion of the intermediate aldehyde to **2** (and possibly the conversion of **3** to **2** as well).

The hypothesized enzymatic conversion of **3** to **2** via the reversible ADH pathway may play a role in the human metabolism of **1**. This suspicion has been preliminarily confirmed by qualitative studies conducted in human liver cytosol in which **3** was converted to **2** in an NAD^+-dependent manner. Specifically, although **3** comprises the same amount (ca. 13%) of total circulatory radioactivity as **2**, **2** and its monooxygenated metabolite **M4** account for ca. 53% of excreted drug-related material while **3** and its metabolite **M5** comprise only ca. 5%. These data when viewed in context of the *in vitro* findings suggest that **3** may be converted to **2** via the reversible ADH pathway (and subsequent ALDH oxidation) *in vivo*, which could result in the majority of drug-related material being excreted in the form of **2** and **M4**, although a contribution of potential differences in volumes of distribution of these metabolites to quantitative differences between excretory and circulatory metabolite profiles cannot be assessed. This phenomenon was also observed in monkeys, but not rats (Shaffer et al., 2005).

Two very minor human metabolic pathways for **1** are its aliphatic hydroxylation to regioisomers **M1** and **M2** and direct conjugation to carbamate **M7**. As opined previously (Shaffer et al., 2005), the site of 4-oxotetrahydroindole hydroxylation is believed to be the same in **M2**, **M4** and **M5** based on CID spectra interpretation, although this was never determined unequivocally. Due to the inconsequential contribution of these two hydroxylated metabolites to the overall human metabolism of **1**, the P450

isoform(s) responsible for their formation, as well as that of the monohydroxylated metabolites of **2** and **3**, were not determined. An in-depth discussion of **M7** formation has also been already undertaken (Shaffer et al., 2005). It is hypothesized that **M7** may form by direct nucleophilic attack of dissolved CO_2 and/or carbonic acid by **1** in circulation; plasma is the lone matrix in which **1** may optimally interact with physiological carbonic acid-dissolved CO_2 pool equilibriums affecting **M7** formation. In humans, total bicarbonate concentrations in plasma tend to be ca. 2-fold greater than that in tissues (Davis et al., 1993), with a fraction (0.5 mM) of plasma CO_2 in carbamate bonds with plasma proteins (White et al., 1968). Furthermore, human venous blood carries approximately a 2-fold greater amount of CO_2 within carbamino bonds than arterial blood (White et al., 1968). Hence, the conditions may be prime for **M7** formation in venal plasma. Whether the formation of **M7** is enzyme-mediated remains to be determined, although **M7** was never observed in any human *in vitro* incubations with [^{14}C]**1**.

Structure elucidation of **U1** and **U2** was elusive. Although these two metabolites each comprised on average ca. 9% of total plasma radioactivity, both were only detected in urine at <1% of administered **1**. These data, coupled with the very short reverse phase LC t_Rs of **U1** and **U2**, suggest these metabolites are highly polar with very low volumes of distribution, which would rationalize them both contributing notably to total circulatory radioactivity and undergoing renal excretion while insignificantly comprising total urinary drug-related material. Such highly polar compounds would not be expected to permeate readily cellular constituents *in vivo* making them of little concern from a safety perspective (Smith and Obach, 2005). It is conceivable that these unidentified,

unionizable metabolites are some type(s) of conjugate(s) that revert(s) to **1** or one of its various metabolites prior to excretion. Metabolites **U1** and **U2** were never observed in any human liver-derived *in vitro* system using [^{14}C]**1**.

Overall, the human metabolism and disposition data suggest both rats and monkeys were appropriate preclinical safety species. Particularly, monkeys most accurately projected the metabolism and disposition of **1** in humans as these species' excretion profiles, metabolite profiles, active renal clearance and pharmacokinetics were essentially identical (Shaffer et al., 2005).

Acknowledgments

The authors acknowledge Neurogen Corporation for their significant contribution to the collaborative development of **1** with Pfizer Inc., and for supplying **1**, **2** and **3**. We thank Dr. Klaas Schildknegt of the Radiosynthesis Group at PGRD, Groton, CT for the synthesis and purification of [^{14}C]**1**, Ms. Beth Obach for conducting excreta and plasma radioanalysis, and Dr. Robert Berman for medical monitoring.

References

Brawman-Mintzer O, Knapp RG, Rynn M, Carter RE and Rickels K (2006) Sertraline Treatment for Generalized Anxiety Disorder: A Randomized, Double-Blind, Placebo-Controlled Study. *Journal of Clinical Psychiatry* **67:**874-881.

Davies B and Morris T (1993) Physiological Parameters in Laboratory Animals and Humans. *Pharmaceutical Research* **10:**1093-1095.

Davis AJ, O'Brien P and Nunn PB (1993) Studies on the Stability of Some Amino Acid Carbamates in Neutral Aqueous Solution. *Bioorganic Chemistry* **21:**309-318.

Drexler B, Grasshoff C, Rudolph U, Unertl K and Antkowiak B (2006) Die $GABA_A$-Rezeptor-Familie. *Anaesthesist* **55:**287-295.

Griebel G, Perrault G, Simiand J, Cohen C, Granger P, Depoortere H, Francon D, Avenet P, Schoemaker H, Evanno Y, Sevrin M, George P and Scatton B (2003) SL651498, a $GABA_A$ Receptor Agonist with Subtype-Selective Efficacy, as a Potential Treatment for Generalized Anxiety Disorder and Muscle Spasms. *CNS Drug Reviews* **9:**3-20.

Hamilton RA, Garnett WR and Kline BJ (1981) Determination of Mean Valproic Acid Serum Levels by Assay of a Single Pooled Sample. *Clinical Pharmacology and Therapeutics* **29:**408-413.

Jarrott B and Iversen LL (1968) Subcellular Distribution of Monoamine Oxidase Activity in Rat Liver and Vas Deferens. *Biochemical Pharmacology* **17:**1619-1625.

Jorgensen TR, Stein DJ, Despiegel N, Drost PB, Hemels MEH and Baldwin DS (2006) Cost-Effectiveness Analysis of Escitalopram Compared with Paroxetine in Treatment of Generalized Anxiety Disorder in the United Kingdom. *The Annals of Pharmacotherapy* **40:**1752-1758.

Kessler RC, McGonagle KA, Zhao S, Nelson CB, Hughes M, Eshleman S, Wittchen H-U and Kendler KS (1994) Lifetime and 12-Month Prevelance of *DSM-III-R* Psychiatric Disorders in the United States. *Archives of General Psychiatry* **51:**8-19.

Lader M (1988) The practical use of buspirone, in: *Buspirone: a new introduction to the treatment of anxiety* (Lader M ed), Royal Society of Medicine Services Limited, London.

Lader M (1994) Benzodiazepines: A Risk-Benefit Profile. *CNS Drugs* **1:**377-387.

Lam RW (2006) Generalized anxiety disorder: how to treat, and for how long? *International Journal of Psychiatry in Clinical Practice* **10:**10-15.

Lee W and Kim RB (2004) Transporters and Renal Drug Elimination. *Annual Reviews in Pharmacology and Toxicology* **44:**137-166.

Lieb R, Becker E and Altamura C (2005) The epidemiology of generalized anxiety disorder in Europe. *European Neuropsychopharmacology* **15:**445-452.

Low K, Crestani F, Keist R, Benke D, Brunig I, Benson JA, Fritschy J-M, Rulicke T, Bluethmann H, Mohler H and Rudolph U (2000) Molecular and Neuronal Substrate for the Selective Attenuation of Anxiety. *Science* **290:**131-134.

Mohler H, Fritschy JM and Rudolph U (2002) A New Benzodiazepine Pharmacology. *The Journal of Pharmacology and Experimental Therapeutics* **300:**2-8.

Olsen RW and Tobin AJ (1990) Molecular biology of $GABA_A$ receptors. *FASEB* **4:**1469-1480.

Rickels K and Rynn M (2002) Pharmacotherapy of Generalized Anxiety Disorder. *Journal of Clinical Psychiatry* **63:**9-16.

Shaffer CL, Gunduz M, O'Connell TN, Obach RS and Yee S (2005) Biotransformation of a $GABA_A$ Receptor Partial Agonist in Sprague-Dawley Rats and Cynomolgus Monkeys: Identification of Two Unique *N*-Carbamoyl Metabolites. *Drug Metabolism and Disposition* **33:**1688-1699.

Sieghart W (1992) $GABA_A$ receptors: ligand-gated Cl^- ion channels modulated by multiple drug-binding sites. *TiPS* **13:**446-450.

Simon N, M., Zalta AK, Worthington III JJ, Hoge EA, Christian KM, Stevens JC and Pollack MH (2006) Preliminary Support for Gender Differences in Response to Fluoxetine for Generalized Anxiety Disorder. *Depression and Anxiety* **23:**373-376.

Smith DA and Obach RS (2005) Seeing Through the MIST: Abundance Versus Percentage. Commentary on *Metabolites In Safety Testing*. *Drug Metabolism and Disposition* **33:**1409-1417.

Testa B (1995a) Dehydrogenation of Alcohols and Aldehydes, Carbonyl Reduction, in: *Biochemistry of Redox Reactions. The Metabolism of Drugs and Other Xenobiotics.* (Testa B and Caldwell J eds), pp 41-69, Academic Press Limited, London.

Testa B (1995b) Oxidations Catalyzed by Various Oxidases and Mono-oxygenases, in: *Biochemistry of Redox Reactions. The Metabolism of Drugs and Other Xenobiotics* (Testa B and Caldwell J eds), pp 298-345, Academic Press Limited, London.

Unzeta M, Castro J, Gomez N and Tipton KF (1983) Comparisons between the Monoamine Oxidase Activities Associated with Mitochondria and Microsomes in Rat Liver. *British Journal of Pharmacology* **80:**622P.

Venkatakrishnan K, Tseng E, Nelson FR, Rollema H, French JL, Kaplan IV, Horner WE and Gibbs MA (2007) CNS Pharmacokinetics of the MDR1 P-Glycoprotein Substrate CP-615,003: Intersite Differences and Implications for Human Receptor Occupancy Projections from Cerebrospinal Fluid Exposures. *Drug Metabolism and Disposition* **35:**1341-1349.

White A, Handler P and Smith EL (1968) *Principles of Biochemistry*. McGraw-Hill Book Company, New York.

Wittchen H-U (2002) Generalized Anxiety Disorder: Prevalence, Burden, and Cost to Society. *Depression and Anxiety* **16:**162-171.

Woods JH and Winger G (1995) Current Benzodiazepine Issues. *Psychopharmacology* **118:**107-115.

Footnote

M.G. current affiliation: Novartis Institutes for BioMedical Research, Department of Metabolism and Pharmacokinetics, 250 Massachusetts Ave., Cambridge, MA 02139.

K.V. current affiliation: Millennium Pharmaceuticals Inc., Department of Clinical Pharmacology, 40 Landsdowne Street, Cambridge, MA 02139.

DMD Fast Forward. Published on January 7, 2008 as DOI: 10.1124/dmd.107.019760
This article has not been copyedited and formatted. The final version may differ from this version.

Legends for Figures

Figure 1. Chemical structure of protonated [^{14}C]**1** (*m/z* 374, * = ^{14}C) and its collision-induced dissociation fragmentation pathway.

Figure 2. Semilogarithmic (top) and linear (bottom) plots of mean plasma concentrations of **1** (▲) and total radioactivity (Δ) in humans.

Figure 3. An overview of the proposed metabolic pathways of **1** in humans. Bold numerical assignments designate observed metabolites; the bracketed structure is a putative metabolite intermediate. [O], enzyme-mediated oxidation; H_2, enzyme-mediated reduction.

DMD Fast Forward. Published on January 7, 2008 as DOI: 10.1124/dmd.107.019760
This article has not been copyedited and formatted. The final version may differ from this version.

Tables

Table 1. Mass recoveries (% of dose) and excretory routes in humans after a single 200 mg oral dose of [^{14}C]**1**

Subject	Urine	Feces	Total
1	28.5	70.5	99.0
2	23.2	78.6	101.8
3	44.3	57.1	101.4
4	22.4	42.1	64.5
5	31.5	66.5	98.0
6	20.4	74.3	94.7
Mean	28.4 ± 8.8	64.8 ± 13.3	93.2 ± 14.3

DMD Fast Forward. Published on January 7, 2008 as DOI: 10.1124/dmd.107.019760
This article has not been copyedited and formatted. The final version may differ from this version.

Table 2. Mean pharmacokinetics of **1** and total radioactivity in humans after a single 200 mg oral dose of [^{14}C]**1**

	1	Total Radioactivity
T_{max} (h)	1.4 ± 0.7	3.2 ± 1.3
C_{max} [a]	355 ± 173	615 ± 152
$t_{1/2}$ (h)	9.2 ± 2.1	7.9 ± 1.5
$AUC_{0-tlast}$ [b,c]	2178 ± 605	5980 ± 1520
$AUC_{0-\infty}$ [b]	2200 ± 607	7428 ± 1275
CL_p/F (mL/min/kg)	23.2 ± 6.0	na
CL_R [d] (mL/min/kg)	2.33 ± 0.85	na
$(CL_R/f_u)/GFR$ [e]	5.8 ± 2.1	na

na: not applicable.

[a]Units are ng/mL and ng-eq./mL for **1** and total radioactivity, respectively.

[b]Units are ng•h/mL and ng-eq.•h/mL for **1** and total radioactivity, respectively.

[c]T_{last} was 48 h for **1** and 24 h for total radioactivity.

[d]Calculated by Ae_{0-48}/AUC_{0-48} and subject weight-normalized.

[e]Plasma free fraction (f_u) was 0.23, GFR was assumed to be 120 mL/min (Davies and Morris, 1993) and subject weight-normalized.

Table 3. Chromatographic and mass spectral data for **1** and its human metabolites.

Compound	LC t_R (min)	$[M+H]^+$ (*m/z*)	CID-generated Fragments[a] (*m/z*)	PC 162[b]	PC 213[c]
1	19.8	374	271, **213**, 193, 180, 162, 86	+	+
U1	4.2	nd	na	—	—
U2	5.5	nd	na	—	—
M1	14.4	390	287, **213**, 196, 178, 86	—	+
M2	15.7	390	287, **213**, 196, 178, 160, 86	—	+
2	16.8	347	329, 180, **162**	+	—
M4	13.8	363	345, 327, 196, **178**, 160, 132	—	—
3	23.6	333	315, 271, 180, **162**	+	—
M5	18.7	349	331, 313, 196, **178**, 160, 132	—	—
M7	27.5	418	400, 374, 271, 239, 213, 180, **162**, 126	+	+

+, $[M+H]^+$ detected; —, $[M+H]^+$ not detected.

nd, not determined due to lack of ionization in either positive or negative ion mode; na, not applicable.

[a]Bold font denotes base peak *m/z* within CID spectrum.

[b]MS response for a precursor ion *m/z* 162 scan.

[c]MS response for a precursor ion *m/z* 213 scan

Table 4. Individual urinary metabolite profiles in humans after a single 200 mg oral dose of [^{14}C]**1**

	% of Dose							
Compound	Subject 1	Subject 2	Subject 3	Subject 4	Subject 5	Subject 6	Mean	SD
1	9.1	9.3	12.9	13.4	7.5	7.3	9.9	2.6
U1	0.4	1.1	—	—	0.8	1.7	0.7	0.7
U2	1.1	—	1.2	—	—	1.2	0.6	0.6
M1	2.0	1.4	6.7	—	1.5	1.2	2.1	2.3
M2	0.1	0.7	1.5	0.7	—	0.6	0.6	0.5
2	7.1	4.4	19.6	5.6	12.5	3.3	8.7	6.2
M4	3.6	2.6	—	1.9	4.3	1.9	2.4	1.5
3	—	—	—	—	—	—	na	na
M5	1.4	1.2	—	0.7	2.4	0.9	1.1	0.8
M7	—	—	—	—	—	—	na	na
Sum	24.9	20.8	41.8	22.3	28.9	18.1	26.1	8.5
Dose excreted[a]	28.5	23.2	44.3	22.4	31.5	20.4	28.4	8.8
^{14}C profiled (%)	87.4	89.4	94.4	99.6	91.7	88.6	91.8	4.5

na: not applicable; —: not detected.

[a]% of dose recovered in urine as reported in Table 1.

Table 5. Individual fecal metabolite profiles in humans after a single 200 mg oral dose of [^{14}C]**1**

	% of Dose							
Compound	Subject 1	Subject 2	Subject 3	Subject 4	Subject 5	Subject 6	Mean	SD
1	14.4	15.9	21.4	7.7	8.7	13.4	13.6	5.0
U1	—	—	—	—	—	—	na	na
U2	—	—	—	—	—	—	na	na
M1	1.8	1.9	1.6	0.5	1.0	2.5	1.6	0.7
M2	—	0.5	—	—	1.0	—	na	na
2	29.3	33.4	25.4	24.9	35.2	38.0	31.0	5.4
M4	10.6	20.2	5.9	6.0	13.3	8.8	10.8	5.4
3	1.3	—	1.4	0.8	1.4	1.2	1.0	0.5
M5	1.6	2.2	1.2	2.2	3.3	5.6	2.7	1.6
M7	—	—	—	—	—	—	na	na
Sum	59.0	74.1	57.0	42.1	64.0	69.5	61.0	11.2
Dose excreted[a]	70.5	78.6	57.1	42.1	66.5	74.3	64.9	13.3
^{14}C profiled (%)	83.6	94.3	99.8	100.1	96.2	93.6	94.6	6.0

na: not applicable; —: not detected.

[a]% of dose recovered in feces as reported in Table 1.

Table 6. Individual circulatory metabolite profiles in humans after a single 200 mg oral dose of [^{14}C]**1**

	% of total ^{14}C $AUC_{0–24}$							
Compound	Subject 1	Subject 2	Subject 3	Subject 4	Subject 5	Subject 6	Mean	SD
1	25.5	19.1	15.7	21.5	19.3	13.5	19.1	4.2
U1	8.9	10.3	6.9	7.1	7.9	8.5	8.3	1.3
U2	—	14.5	7.5	11.1	9.5	13.5	9.4	5.2
M1	—	—	—	—	—	—	na	na
M2	3.6	2.5	3.4	1.1	1.8	3.1	2.6	1.0
2	11.1	11.2	23.1	10.4	14.2	6.9	12.8	5.6
M4	5.7	6.2	7.5	3.3	7.7	5.0	5.9	1.7
3	11.5	17.6	10.1	14.6	8.6	12.1	12.4	3.2
M5	—	—	—	—	—	—	na	na
M7	1.8	1.1	—	1.3	0.8	0.8	0.9	0.6
^{14}C profiled (%)	68.0	82.5	74.3	70.4	69.8	63.4	71.4	6.5

na: not applicable; —: not detected.

DMD Fast Forward. Published on January 7, 2008 as DOI: 10.1124/dmd.107.019760
This article has not been copyedited and formatted. The final version may differ from this version.

Table 7. Metabolite profiles in human hepatic *in vitro* systems using [^{14}C]**1** (20 μM)

System	Compound[a] (% of total ^{14}C)				
	1	**M1**	**2**	**3**	**M5**
HLMs					
+NADPH	61	7	8	14	9
-NADPH	51	—	13	36	—
Hepatocytes	57	—	32	11	—
Mitochondria	76	—	17	6	—

—: not detected.

DMD Fast Forward. Published on January 7, 2008 as DOI: 10.1124/dmd.107.019760
This article has not been copyedited and formatted. The final version may differ from this version.

Table 8. Initial oxidation rates of **1** (20 μM) to **2** and **3** in recombinant human MAO-A and MAO-B membranes

System	Velocity[a] (pmol metabolite/min/mg protein)		
	2	**3**	**2** + **3**
MAO-A	0.581	0.542	1.124
MAO-B	3.051	31.806	34.857
MAO-B/MAO-A	5	59	31

[a]Each velocity is an average of two incubations.

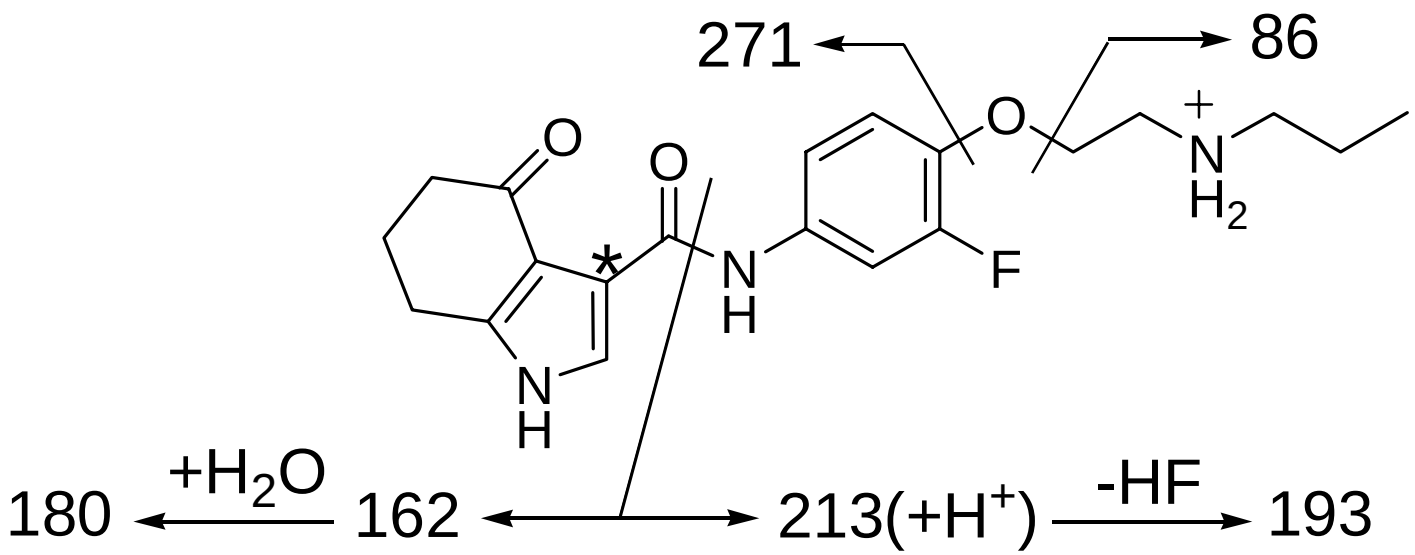

Figure 1

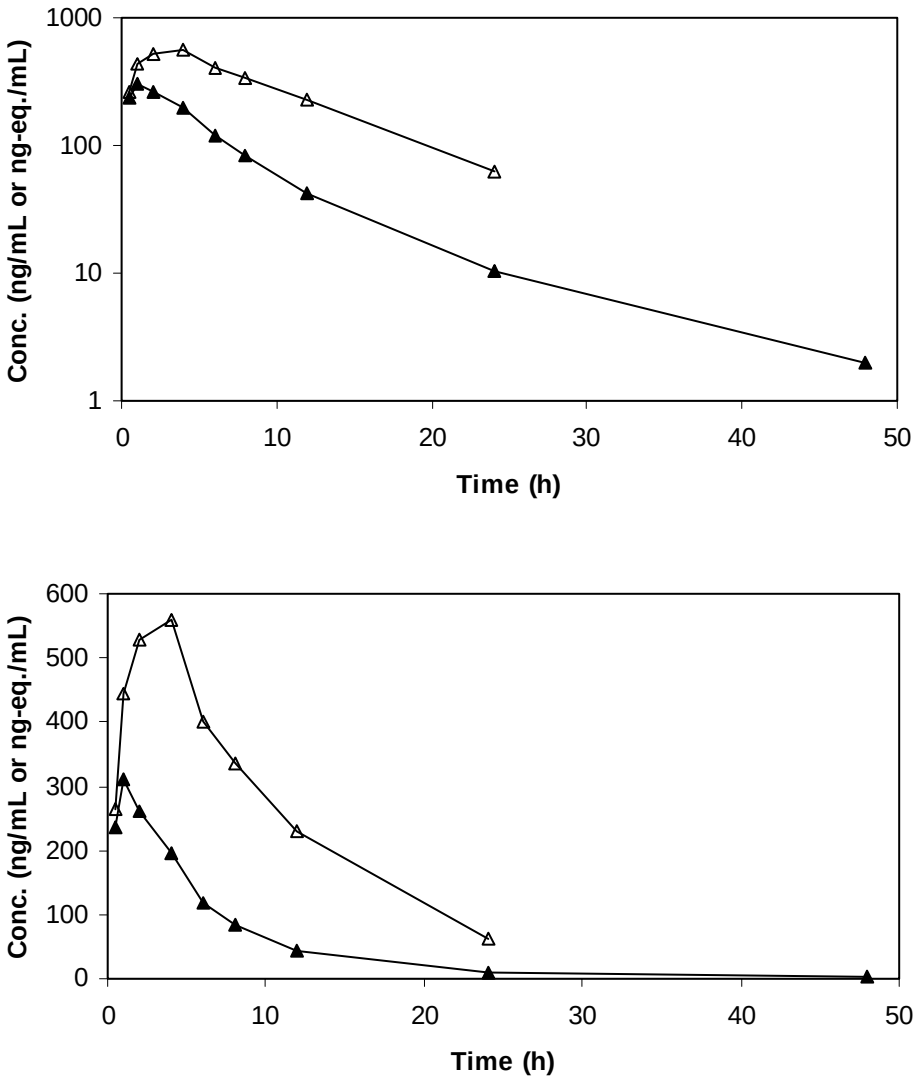

Figure 2

DMD Fast Forward. Published on January 7, 2008 as DOI: 10.1124/dmd.107.019760
This article has not been copyedited and formatted. The final version may differ from this version.

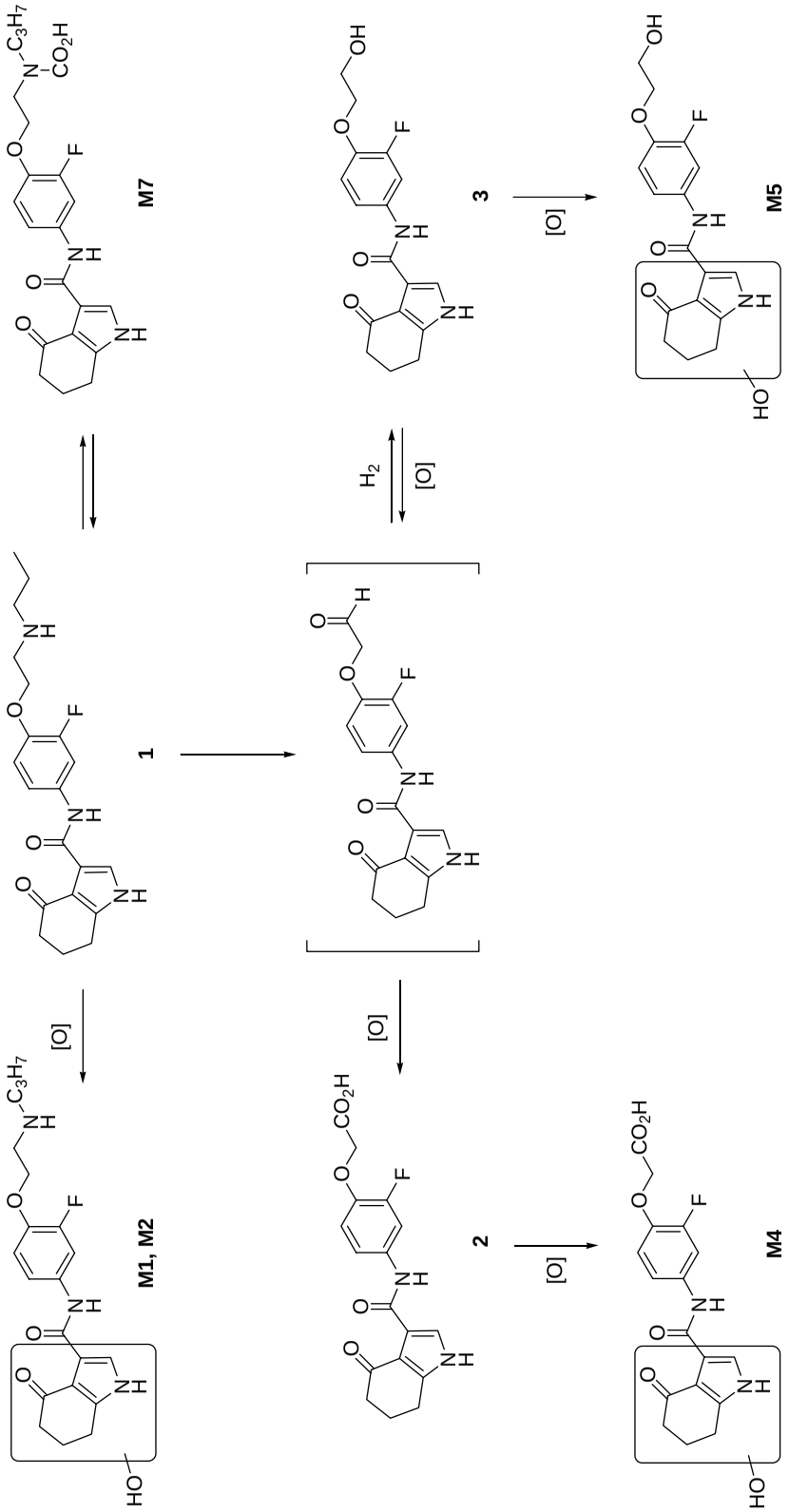

Figure 3